Nano Size Hexagonal Ferrites For Microwave and Millimeter-Wave Devices

Mohammed N. Afsar[1] and Wei. Quan[1]

[1]Department of Electrical and Computer Engineering, Tufts University, Medford, MA 02155, USA

Complex dielectric and magnetic properties of micro- and nano-size hexagonal ferrites have been studied. Two different measurement techniques have been applied to characterize the samples in the broad frequency range from 1.7 GHz to 120 GHz. It was observed that the constitutive material properties, namely permittivity and permeability, as well as the ferromagnetic resonance frequency of the samples vary with the change in particle dimensions. Based on the results of these measurements, a model for calculating the ferromagnetic resonance frequency of ferrite powders has been derived, which takes into account the size and shape of the particles in the sample. It can be concluded from the size-dependent absorption properties observed in this study that these materials show promise as tunable millimeter wave absorbers.

***Index Terms*—Dielectric permittivity, ferromagnetic resonance, magnetic domains, magnetic permeability, nanoferrites.**

I. Introduction

THE PROPERTIES of a material change as its physical size shrinks, due to the increased percentage of atoms on the surface of the material. For a given amount of material, the surface area compared to the volume increases as the particle size decreases. Thus the proportion of constituent atoms on or near the surface increases. For instance, consider a microparticle with a radius of 30 μm and surface area of 0.01 mm^2. The same mass of this material in nanoparticulate form, with each particle having a radius of 30 nm will consist of 1 billion nanoparticles, with a total surface area of 11.3 mm^2. Thus compared to microparticles, nanoparticles have a very large surface area and higher number of particles per unit mass [1]. This feature is important because many reactions occur on the surfaces of materials. The small particle form of a material may have properties quite different from its properties in bulk form.

Microwave ferrite devices are used to control energy propagation by a static or switchable dc magnetic field [2]. Another application of ferrites is in frequency tuning of electronic components, which has traditionally required external magnets. However, at high frequencies, the magnetic bias required increases the size and cost of the components. This can be avoided by using self-biased hexaferrites that have high effective internal magnetic anisotropy that can provide the permanent magnetic bias [3], thus eliminating the need for bulky external magnets.

Electromagnetic interference (EMI) suppression is needed for radar targets and in electronic devices that are densely packed. Factors such as thickness, weight, mechanical strength and environmental conditions limit the choice of available absorbing materials. As the clock speeds of electronic devices approach microwave frequencies, it has become essential to study the high frequency properties of the materials used in electronics devices and components. Reduction in component size would result in faster speed and higher density of logic on processors and circuit boards. Further, due to the significant increase in the density of components in electronic systems such as high-speed digital interfaces in computers, digital cameras, scanners, and so forth electromagnetic interference becomes a serious issue. Special materials are used in the design of circuits and packaging applications to ensure electromagnetic compatibility in the smaller designs [4]. For the case of narrow-band absorbers, an optimum solution would require a compromise between absorber thickness and absorption characteristics. Material parameters can be optimized once the intrinsic material properties are known. In the case of wide band absorbers the number of parameters increases and optimization becomes a complex task. Such a design can be greatly simplified by using electromagnetic simulation tools. But the accuracy of the results from such simulations is determined by the accuracy with which the material properties are known. In the development of computer aided design circuit simulation programs, both magnitude and phase data are required for accurate models. Therefore if the exact dependence of material properties on frequency is known, application specific absorbing materials can be designed. The intrinsic material properties have been used to study the microwave power absorption of ferrites [5] and magnetic loss in microwave heating [6].

Microwave remote sensing is another field where material characterization plays an important role. In remote sensing, materials are identified by studying the reflection and scattering of microwave signals by the target specimens [7], which in turn depend on the constitutive properties of the target material. Thus by characterizing materials and creating a database, identification of materials by remote sensing can be done more efficiently.

There is a novel application of nanoferrites in magnetic resonance imaging. In MRI, the person under examination is exposed to a RF pulse in the presence of an external magnetic field. The resulting changes in the spin of the protons in water molecules are used to construct a three dimensional image of the subject. Use of the magnetic nanoparticles in biological systems can enhance the detection sensitivity [8]. Nanomaterial tubes are ideal probe tips for scanning microscopy due to their small diameter which maximizes the resolution and high aspect ratio [9]. With further improvement in imaging technology, magnetic nanoparticles exhibiting

strong resonances can be used to perform localized imaging. The scope of applications for nanopowders has driven the need for extensive research in this field.

The applications of nano-ferrites in RF and microwave appications have been studied and reported [10]. Precise characterization of materials is required for applications listed above. To understand and predict the behavior of magnetic and dielectric materials, the measurement data of intrinsic material properties is essential.

Over the last 50 years, many devices have been developed across the microwave spectrum. However, many challenges remain to be addressed to meet the demands for miniaturization, broader bandwidths, higher operating frequencies and reduced costs [2]. From the discussion in the previous section it is evident that the knowledge of material properties is indispensable for the development of novel applications in the fields of electronic and biomedical engineering. Characterization of constitutive material properties allows scientists to understand, analyze and modify the behavior of the materials. This also provides the flexibility to tailor the material properties according to the application. However, higher frequencies of operation and smaller sizes of the samples make characterization challenging. The measurement methodology is limited by the size of components needed to make measurements at such high frequencies and also by the sensitivity of the measurement set-up to interference from other sources. Any additional length of cables or connectors adds significant delay and phase change at high frequencies.

The properties of materials depend on the frequency of the application, size and composition of the sample. Controlled growth of powdered ferrites is difficult and as a result the final size and shape of the particles may be different from what was intended. Physical properties of nanoparticles are influenced significantly by the manufacturing technique [11], [12]. The preparation conditions such as chemical composition, sintering temperature and amount of substitutions have been known to affect the physical properties of the fabricated material. Therefore, in materials research and engineering, microwave techniques for the characterization of material properties can be used as nondestructive testing tools to check if the final products match the specifications that they were designed for. Distribution of particle sizes and inter particle spacing affect the magnetic properties. Therefore, it is important to know the effect of particle size on the material properties. In order to do so, it is necessary to collect data for nanopowders of different sizes and analyze the relationship between their size, composition, morphology and their electromagnetic responses. One of the critical challenges faced currently by researchers in the field of nanotechnology is the lack of instruments to characterize and manipulate the materials prepared at the nanometer level. Needless to say that characterization of nanopowders requires extreme sensitivity and accuracy.

Furthermore, the particles in the powdered samples tend to form aggregates. These aggregates can vary in size from a few nanometers to micrometer. It may not always be possible to avoid aggregate formation. Therefore it is essential to check the state of the sample during measurement and perform controlled measurements.

Constitutive material properties of powdered ferrite samples are studied in this work. Materials have been studied in solid form in the past. However, here the samples are studied as pure powders, without the need to form solid samples by diluting them with epoxy or other forms of conductive binder. Two different measurement techniques have been applied to characterize the samples in the broad frequency range from 1.7 GHz to 120 GHz. For microwave measurements, covering frequencies between 1.7 GHz to 40 GHz, a transmission/reflection based measurement technique has been used to obtain the intrinsic material properties. A vector network analyzer is employed to measure the s-parameters of the material under study. Rectangular waveguides are used to connect the sample to the measurement ports of the network analyzer. The measured data is used to calculate the complex dielectric permittivity and magnetic permeability of the samples.

For the millimeter wave measurements, a quasi-optical high frequency spectrometer is used. Backward wave oscillators are used as the high frequency power sources. The signal propagates through two channels. The optical path, consisting of horn antennas and lenses to guide the Gaussian beam, is used for the measurement and the other channel made up of high frequency components such as directional couplers and attenuators acts as the reference path. Power is divided between these two arms by using a waveguide-based directional coupler. The permittivity and permeability values are derived from the transmission data of the sample using curve fitting functions. A thorough error analysis has been attempted to identify the possible sources of errors.

The samples investigated in this work include M-type hexaferrites, spinels and perovskite ferrites. Hexaferrite samples with identical material composition but different particle sizes are used. The study revealed a dependence of material properties of hexagonal ferrites on the morphology of the particles in the powdered sample. The morphology of the samples was studied using scanning electron micrographs (SEM) and their compositions were verified using X-ray diffraction. The possible reasons for the difference in behavior of nano-powder and micro-powder samples are suggested. A calculation model has been defined to determine the resonance frequency for such samples. The proposed model takes into account the structural properties of the particles in the sample. The results indicate that it is possible to use the hexaferrites as high frequency tunable absorbers.

II. Experimental Set-Up

The materials studied here were commercially available samples of barium hexaferrite ($BaFe_{12}O_{19}$) and strontium hexaferrite ($SrFe_{12}O_{19}$) consisting of micro-sized and nano-sized particles in powdered form. Therefore, a total of four different samples were studied. Due to the hexagonal symmetry of the structure, such ferrites have a major preferred axis, i.e., there are certain preferred directions along which it

is easier to magnetize the material. This makes them highly anisotropic. According to the manufacturer data sheet, the average particle size was between 50-100 nm for the nanopowder and less than 10 µm for the micropowder. Each measurement technique is explained in detail in the following sections.

A. Microwave measurement technique

Microwave measurements covering the frequency range from 1.95 GHz to 40 GHz (consisting of eight frequency bands) were carried out using transmission reflection based waveguide technique. The technique was developed by Nicolson, Ross and Weir, has been extensively used for studying solid samples in the past years [13]. The sample is loaded between the waveguides and the s-parameters of this two port network are measured using a network analyzer. Several algorithms have been suggested to derive material properties, such as magnetic permeability and electrical permittivity from this data [13], [14]. The algorithm used to determine the permittivity and permeability from the measured data has been modified over the years to improve accuracy. A modified algorithm was used here to derive the electromagnetic properties of powdered samples. It eliminates the need of using guess parameters or iterative calculations. The phase of the measured parameters and reflection coefficient is resolved by applying phase unwrapping technique. The cut-off frequency for each frequency band is used in calculating the reflection and transmission coefficients, which are used to calculate the permittivity and permeability of the sample. a schematic diagram of the measurement set-up is shown in Fig. 1.

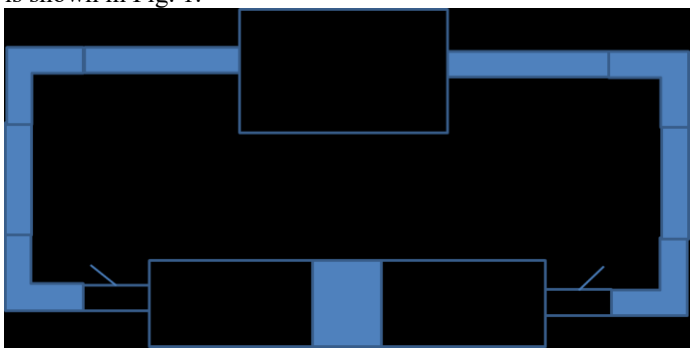

Fig. 1. Block diagram of the measurement setup

In this arrangement, the sample is inserted between the two waveguides. Since the sample is in powder form, a lossless tape is used at the walls of the sample holder to keep the powder from falling. The other ends of these waveguides are connected to the network analyzer by a coaxial cable. One limitation in this measurement technique is that the area of the sample holder is fixed, being dictated by the waveguide size defined for each frequency band. For instance, the waveguide dimensions for X band (8.2 GHz – 12.4 GHz) are 0.9 x 0.4 inch whereas the dimensions for Ka (26.5 GHz – 40 GHz) band are 0.28 x 0.14 inch. Due to the size restriction and varying dimensions of the sample holder, it is difficult to maintain uniform density of the sample across the eight frequency bands. However, the thickness of the sample inside the sample holder can be varied. The powdered sample was filled inside the sample holder such that the sample density could be maintained as close to the adjacent bands as possible. As a result, the sample would not completely fill the sample holder and an air gap was created, as shown in Fig. 2. The presence of the air gap was taken into account in the algorithm used to derive permittivity and permeability values. On order to do this, the measured s-parameters were modified as shown below in (1),

$$\tilde{S}_{11} = S_{11} e^{\left(l \times \sqrt{k_0^2 - k_c^2}\right)}$$

$$\tilde{S}_{21} = S_{21} e^{\left((l-d) \times \sqrt{k_0^2 - k_c^2}\right)}$$

where, l is the quarter wavelength difference between *thru* and *line* in air, d is the thickness of the sample inside the waveguide, k_0 is the wavenumber of the sample and k_c is the cutoff wavenumber. These values were used in the algorithm to derive the permittivity and permeability values.

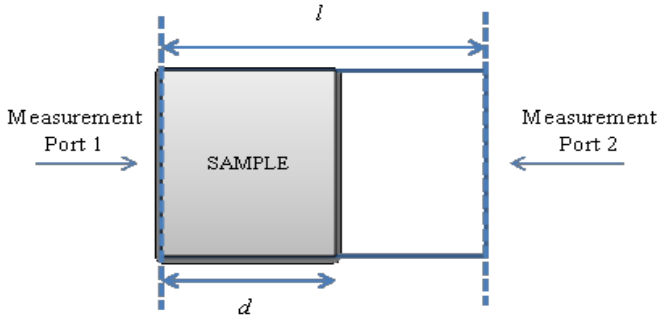

Fig. 2. Sample holder, width l, partially filled with sample, thickness d. The waveguides are connected at ports1 and 2.

Although there was strong agreement in data obtained at the end of one band and beginning of the next band, slight variations were observed in a few measurements, which could be due to different densities. When combining the data across the eight bands, second and sometimes third order mathematical curve fitting functions were used to account for this effect.

The final form of the equations used to derive permittivity and permeability values is given below,

$$\varepsilon = -j\left(\frac{c}{f}\right)^2 \left(\frac{1-\Gamma}{1+\Gamma}\right)\left(\frac{1}{2\pi d}\right)\left(\ln\left(\frac{1}{|T|}\right) + j(2\pi n - \varphi_T)\right)\left(\sqrt{\left(\frac{1}{\lambda_0}\right)^2 - \left(\frac{1}{2a}\right)^2}\right) \quad (2)$$

$$\mu = \frac{\eta\gamma_{TE_{10}}}{j\gamma^0_{TE_{10}}} = -j\left(\frac{1+\Gamma}{1-\Gamma}\right)\left(\frac{1}{2\pi d}\right)\left(\frac{\ln\left(\frac{1}{|T|}\right) + j(2\pi n - \varphi_T)}{\sqrt{\left(\frac{1}{\lambda_0}\right)^2 - \left(\frac{1}{2a}\right)^2}}\right) \quad (3)$$

where, Γ is the reflection coefficient, T is the transmission coefficient, γ_{TE10} and γ^0_{TE10} are propagation constant for the TE_{10} mode with and without the material inserted in the waveguide, a is the longer dimension of the rectangular waveguide, ϕ_T is the phase of transmission coefficient and d is

the material thickness.

B. Millimeter wave measurement technique

Measurements in the frequency range from 40 GHz to 120 GHz were carried out using free space millimeter wave quasi optical spectroscopy. The transmittance spectrum was studied to observe the resonance frequency and derive the permittivity and permeability of the sample [14]. A quasi-optical backward wave oscillator was employed to measure the variation of the power transmittance of Barium and Strontium hexaferrite micro- and nano- powders. These materials show strong ferromagnetic resonances in the millimeter wave frequency range. The permittivity and permeability values are obtained by comparing the measured power transmittance spectra of these samples with the theoretically obtained spectra. By using appropriate BWO source and waveguide elements such as directional couplers, phase shifters and antennas, the power transmittance spectrum of the sample is measured in three frequency bands, namely, Q (34-56 GHz), V (44-76 GHz) and W (70-117 GHz) bands.

The block diagram of the measurement set-up is shown in Fig. 3. The high power backward wave oscillator source is used to generate the millimeter waves. As seen in the block diagram, the modulated signal is divided into two channels. Instead of using a pure optical technique, which has been reported to have high measurement error [15], the measurement system developed here uses a guided wave technology combined with a quasi-optical millimeter wave system for precision measurements. One of the channels is made up of the waveguide components to serve as a reference for phase information. The other channel consists of an optical transmit and receive system. The two signals are combined at the detector and the interference of the combined waves is recorded with a detector. Specially written Lab View based software is used to automate the spectrometers and process the measured data. Horn antennas are used to radiate and receive energy.

The quasi-optical channel is placed inside the pole pieces of a 1 Tesla magnet to attain partial saturation of the magnetization in the samples. The material under study is placed in the common focal planes of the lenses on its two sides. The powders were carefully packed inside the sample holder. The sample holder is made out of aluminum frame with mylar films fixed through Teflon strips on either side. The thickness of the sample holder is 12 mm. The thickness of mylar sheet is 0.05 mm. Prior to filling the sample holder, the powdered samples were manually milled to make sure that the sample does not form agglomerates. For both measurement techniques, the powders were carefully packed inside the sample holder in gradual amounts to make sure that there are no air gaps within the sample.

The computer controlled quasi-optical measurement system records the power transmission spectrum of the sample under test and the permeability and permittivity of the sample are extracted from this spectrum by fitting the theoretical curves to the experimental ones. The reference data is collected by running the set-up without placing any sample between the lenses. Next, the same procedure is repeated with the sample located in its position in the optical channel. The power transmittance spectrum is then obtained as the ratio of the measured point to point voltages at the detector with and without the sample. First, the curve fitting techniques are applied to fit the calculated transmittance spectrum to the measured transmittance spectrum. From this curve fitting, the values of real and imaginary parts of permittivity are determined. Next, the permeability is determined by using Schloemann's equation,

$$\mu_{eff} = \frac{1}{3} + \frac{2}{3}\left[\frac{(\omega/\gamma)^2 - (H_a + 4\pi M_s)^2}{(\omega/\gamma)^2 - H_a^2}\right]^{\frac{1}{2}} \qquad (4)$$

The values of saturation magnetization (M_s,) and effective anisotropy (H_a) in this equation are also evaluated from the curve fitting program by using the known values of real and imaginary parts of the permittivity.

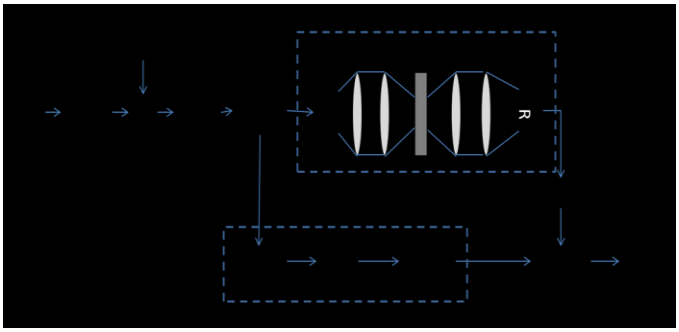

Fig. 3. Spectrometer for measuring the transmission characteristics of the material at millimeter wave frequencies.

III. Results and Discussion

The results of the measurements described in the previous sections are presented and discussed in this part. A considerable amount of useful information can be derived from these results. In addition to the permittivity and permeability values of a number of ferrite materials, the loss factor and reflection coefficient of the samples are also obtained. These characteristics help predict the possible use of these materials in different applications such as the radar absorbing materials and microwave filters. Wherever published data is available in literature, the properties of the nano-powders have been compared with the properties for the same composition of samples in bulk form. A few deviations from the expected results have been observed. By controlling the material type (dielectric or magnetic) and its thickness, loss factor, impedance and internal design, the performance of a microwave absorbing material can be optimized for a single narrow band frequency, multiple frequencies, or over a broad frequency spectrum.

A brief description of the nanopowders analyzed in the microwave and millimeter wave frequency ranges is enumerated in TABLE I. The particle sizes mentioned in this table are as per the manufacturer's data sheets. In addition to these samples, a solid sample of Teflon was also studied using

the waveguide technique in each frequency band. This is used as a reference material to validate the ability of the proposed algorithm for determining the permittivity and permeability values from the measured s-parameters. Powders of barium ferrite and strontium ferrite consisting of micro-size particles were also studied to observe if the differences in the properties of the nano- and micro-size ferrites can be detected using the proposed measurement technique.

TABLE I
LIST OF NANO-SIZE POWDERS INVESTIGATED

Sample	Chemical Formula	Sample Description
Barium nano-ferrite	BaFe12O19	Avg. particle size 50-100 nm
Barium micro-ferrite	BaFe12O19	Avg. particle size 5-50 μm
Strontium nano-ferrite	SrFe12O19	Avg. particle size 50-100 nm
Strontium micro-ferrite	SrFe12O19	Avg. particle size 5-50 μm

Micro-size Barium and Strontium ferrite samples were purchased from Trans-tech, Inc.

The powders are filled inside the sample holder that is placed between the waveguides. A transparent tape is used on one side of the sample holder to prevent the powdered sample from falling off. The use of tape does not affect the measurement results. This was verified on the solid Teflon sample. The sample holders used in the measurement process are shown in Fig. 4. Sample holders for G, C and Ku frequency bands are shown here.

Fig. 4. Empty sample holders used for the measurement of G, C and Ku frequency bands.

A. Microwave measurement result

The generic formula for M-type ferrites is MO.6Fe2O3, where M can be any divalent ion. The two hexaferrite samples studied here are barium (BaO.6 Fe2O3 or BaFe12O19) and strontium hexaferrites (SrFe12O19). Compared to ferrites with inverted spinel or garnet structures, hexagonal ferrites have larger intrinsic magnetic fields. Due to the hexagonal symmetry of the structure, such ferrites have a major preferred axis, i.e., there are certain preferred directions along which it is easier to magnetize the material. This makes them highly anisotropic. As a consequence of the effectively large internal magnetic anisotropy, these materials remain magnetized even after the external applied field is removed. This diminishes the need for an external magnetic field and makes M-type hexagonal ferrites very useful in the design of high frequency devices. Bulk hexagonal ferrite samples have been extensively used in microwave applications such as transformers and circulators. Due to the growing interest in these materials, the basic characteristics of nano-sized M-type hexaferrite powders have been extensively studied [16].

Recently these materials are also being investigated for use as microwave absorbers [17]-[20] due to their large magnetic losses in the microwave range. The hexagonal ferrites are suitable as radar absorbing materials due to their large permeability values and favorable dielectric properties at microwave frequencies. Several substituted barium hexaferrite samples are being designed for such applications [21]-[24]. Substitution for the Fe^{3+} and Ba^{2+} ions is an effective method to vary the magnetic properties of barium hexaferrite. Common substitutions include Zn-Ti, Ni-Zr or Ti-Cu. It has been found that the absorption properties can be manipulated by varying the amount of substitution [25].

The permittivity and permeability of these materials have been extensively studied in bulk form [26]. When materials are produced in powder form, depending on the particle size, the microwave behavior may change. However, not much has been reported on these materials in powder form. This could be due to the lack of accurate high frequency characterization techniques suitable for the powder samples.

The variation of the real and imaginary parts of the permittivity and permeability of barium hexaferrite nanopowders at microwave frequencies are shown in Fig. 5. The average values over certain frequency range have been calculated and used to generate these plots. Data of 201 points for every frequency band have been measuered and reported, and thus there are a group of 1608 points have been posted. Among the entire data collection, the certain selective frequency point are marked on these plosts. Compared to the reported values of real part of permittivity of bulk barium hexaferrite [27], [28], the measured data of nano-powders are much smaller. These numbers refer to the real part of the permittivity. The real part of the permeability of barium hexaferrite in bulk form has been reported to be as high as 6 [27]. It should be noted that the bulk properties are reported for solid samples whereas the samples studied here are being measured in powder forms. The permittivities for M-type barium and strontium ferrites in bulk form have been reported in literature to lie between 14 and 16 [28], [29]. These are significantly different from the values measured here for their powder samples.

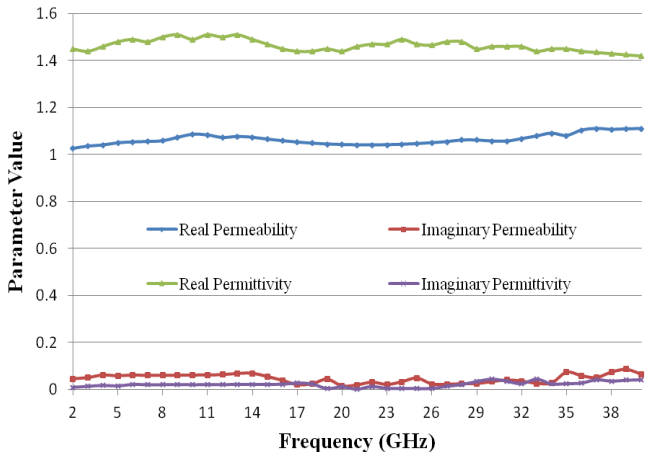

Fig. 5. Variation of permeability and permittivity of barium hexaferrite nano-powder with frequency. The average values of the imaginary permittivity and permeability are 0.0516 and 0.0706, respectively.

For barium ferrite, the calculated average values of the real and imaginary parts of the permeability are 1.06 and 0.07 respectively for sample density of 0.4g/cm^3. For the same sample, the average permittivity values are 1.46 and 0.05 respectively. The real part of permeability stay steady constant over the selected frequency range except a drop at Ka band while the real part of permittivity vary slightly. A little variation of measured values is observed at the extremities of some bands. This performance shows a discontinuity between bands boundary in the plots of measured points. Because of the sample used for measurement at different frequency have same density; the difference of plotted data is small between bands.

The non-zero values of the imaginary parts of permittivity and permeability suggest that the ferrites are lossy in nature. This means that an electromagnetic wave propagating through these materials would lose energy. This is an essential property for absorbing materials. The dielectric and magnetic loss tangent values for each sample are listed in TABLE II. Another important observation here is that the permittivity and permeability values are very close to each other. This means that the impedance seen at the front end of the material would be close to the free space impedance (377 ohm) and hence there will be very little reflection at the air-ferrite interface. This satisfies the first condition for the absorbing materials and thus these powders may be useful as non-reflecting coatings for microwaves. The impedance values shown here have been calculated from the permittivity and permeability values using the following equation,

$$Z = \sqrt{\frac{\mu}{\varepsilon}} = 120\pi \sqrt{\frac{\mu_r}{\varepsilon_r}} \qquad (4.1)$$

The frequency dependence of impedance thus obtained is shown in Fig. 6. It can be observed that the front end impedance of barium ferrite nanopowder approaches the free space impedance value of 377 ohm towards the high end of microwave frequencies.

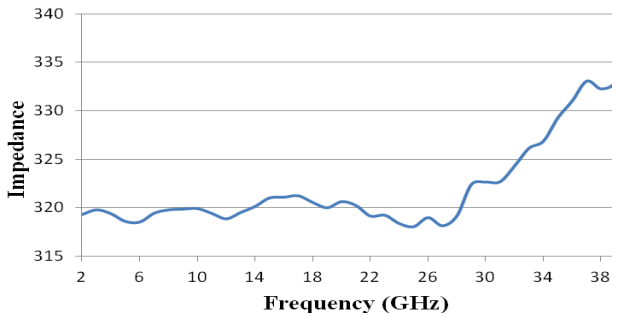

Fig. 6. Variation of front-end impedance of barium hexaferrite nano-powder with frequency

Bulk barium hexaferrite is known to have resonance frequency around 48 – 50 GHz [28]. Results of our measurement on ferromagnetic resonance frequency of Barium hexaferrite powder are presented later. It suffices here to state that resonance reqeuncy of barium hexaferrite powder also falls within the above range. The resonance corresponds to the maximum absorption frequency of the sample. From the data presented here, it can be predicted that nano size-barium ferrite should be an excellent microwave absorbing material at relatively lower frequencies, near the higher end of Ka band. In order to better understand the performance of the sample as an absorber, we calculate the front end reflectance. The front end reflectance has been shown to have the form,

$$\Gamma = \frac{Z_2 tanh(j\gamma d) - Z_1}{Z_2 tanh(j\gamma d) + Z_1} \qquad (4.2)$$

Here, medium1 is air and medium 2 is nano-size barium ferrite powder. The power reflection coefficient Γ, when multiplied by the incident energy gives the amount of energy that gets reflected from the air-sample interface due to impedance mismatch between the two media. Fig. 7 gives the frequency dependence of Γ. This behavior is as expected. As the front end impedance becomes close to 377 ohm, the reflected energy decreases considerably. At frequencies higher than 34 GHz, the reflectance is less than -10dB, which is a practical value for an absorber. The performance improves significantly beyond 38 GHz with power reflection coefficient touching -25 dB at 38 GHz. Plots 4.3 and 4.4 are mutually consistent and suggest that Barium hexaferrite nanopowder should have excellent non-reflecting properties at higher frequencies. The magnetic loss shows an increase. The real part of permittivity decreases in magnitude, becoming closer to the permeability value near the frequency of resonance. The reflectivity results shown below are for a sample of thickness of 2 cm.

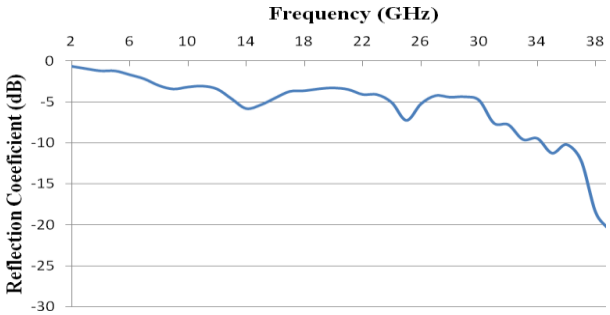

Fig. 7. Variation of reflectance of 2cm thick sample of barium hexaferrite nano-powder with frequency.

The properties of strontium hexaferrite nanopowder are discussed next. Fig. 8 shows the variation of permeability and permittivity of strontium hexaferrite nanopowder with frequency. The overall variation pattern in this case is quite similar to the one found for the corresponding barium based nanopowder (Fig. 5). The values of the permittivity and permeability are somewhat higher for the strontium nanopowder than for the barium nanopowder. The average values of real parts of permittivity and permeability obtained for strontium hexaferrite are 1.689 and 1.088, respectively. Further, the real part of the permeability of strontium hexaferrite nanopowder does not vary much with frequency except perhaps towards the higher end of frequencies used in our measurements. The magnetic loss factor for the strontium

nanopowder shows a minor increase towards the higher end of the frequency range. The imaginary part of permittivity is very small and would not contribute much towards absorption in this case for the strontium nanopowder. However, the magnetic loss is considerably higher. We can therefore expect significant energy attenuation during propagation in strontium hexaferrite nanopowder.

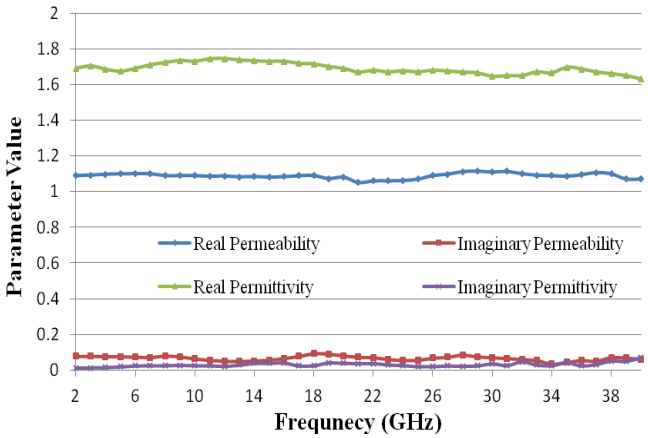

Fig. 8. Variations of permittivity and permeability of strontium hexaferrite nano-powder with frequency.

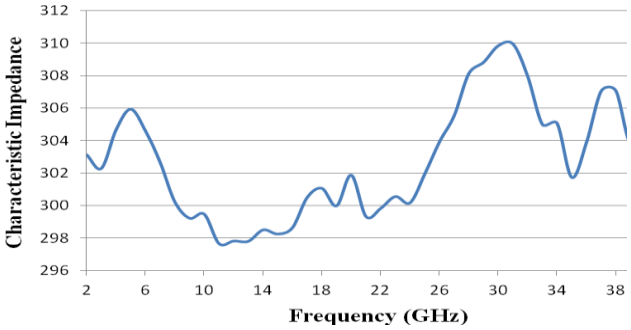

Fig. 9. Variation of front-end impedance of strontium hexaferrite nano-powder with frequency.

The difference between real parts of permittivity and permeability of Strontium hexaferrite nanopowder is small but somewhat larger than what was observed for barium hexaferrite nano-powder. As a result, its characteristic impedance in this frequency range is not as close to the free space impedance value of 377 ohm as it was in the case of barium hexaferrite nanopowder. The variation of impedance of strontium hexaferrite nano-powder with frequency is shown in Fig. 9. In this frequency range, the highest impedance value is 310 ohm at about 30 GHz. The fluctuation in values after that frequency could be due to measurement inaccuracies. But it can be concluded that the impedance rises towards the end of the frequency range investigated here, just as in the case of Barium hexaferrite nanopowder.

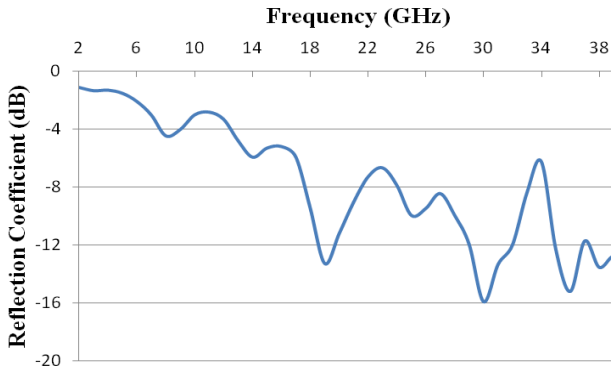

Fig. 10. Variation of reflectance of 2cm thick sample of barium hexaferrite nano-powder with frequency

The results of measurement for the two nano-size hexaferrites are summarized in TABLE II. The data in this table provide only the average value of each parameter across the wide frequency range from 2 to 40 GHz.

It is clear from Fig. 5 and Fig. 8 that the parameter values are somewhat frequency dependent. For instance, the dielectric loss tangent value is very small at lower frequencies but increases steadily with frequency. This behavioral phenomenon cannot be captured in average values and thus the frequency dependent analysis is essential. A single average value for any parameter undermines the fact that the value is high at certain frequencies and falls at others.

The variation of power reflection coefficient for Strontium hexaferrite nanopowder shown in Fig. 10 is in general agreement with its impedance values. The impedance was observed to be best matched at 30 GHz and this corresponds to the sharp -16 dB minimum in reflectance observed in Fig. 10.

For comparison, micro-size samples of Barium hexaferrite were also studied. The frequency dependence of real and imaginary parts of permittivity and permeability for this powder is shown in Fig. 11. The average value of real parts of permittivity and permeability for the micro-size sample were found to be 3.065 and 1.1069, respectively. An interesting observation here is that the values for the micro-size powders are different from those measured for the nano-size powder.

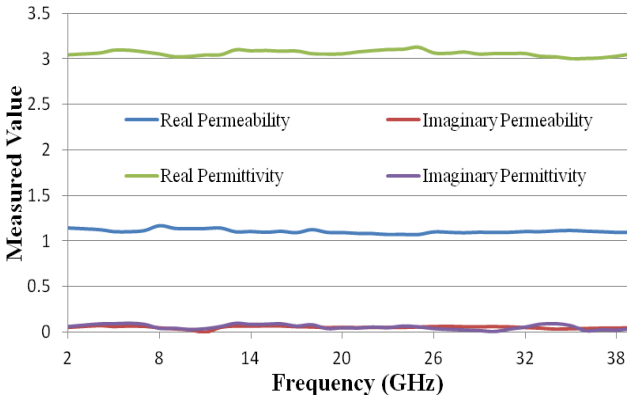

Fig. 11. Material properties of Barium ferrite micro-powders are shown. The average value of real and imaginary parts of permittivity is observed to be 3.065 and 0.0559 whereas real and imaginary parts of permeability are 1.1069 and 0.0536, respectively.

TABLE II
DIELECTRIC AND MAGNETIC PROPERTIES OF HEXAFERRITE NANOPOWDE

Material	Dielectric Permittivity			Magnetic Permeability			Density (g/cc)	Bulk Permittivity
	Real Part	Imaginary Part	Loss Tangent	Real Part	Imagin-ary Part	Loss Tangent		
Barium Hexaferrite	1.464	0.052	0.016	1.064	0.071	0.041	0.4004	16 [28]
Strontium Hexaferrite	1.689	0.030	0.018	1.088	0.0658	0.060	0.3531	14 [29]

B. Millimeter wave measurement result

The power transmittance spectra of micro- and nano-powders of Barium and Strontium hexaferrites were obtained in the millimeter range using the quasi-optical technique described in the previous section. Complete information on the permeability and permittivity of the samples can be obtained from the measured variations in the power transmittance of Barium and Strontium hexaferrite powders by Schloemann's equation.

The best fit results for nano- and micro-sized Barium ferrite samples in the millimeter wave frequency range are shown in Fig. 12 and Fig. 13, respectively. The phenomena of ferromagnetic resonance can be seen more clearly in these plots. It should be noted here that Schloemann's equation is useful in calculations close to the ferromagnetic resonance frequency. However, as we move away from the resonance frequency, the accuracy of this method decreases. In fact, for frequencies that are distant from the resonance frequency, more accurate calculations can be performed by using Polder's theory [30]. Therefore, the permeability data that is presented in the following plots is not accurate at higher frequency points.

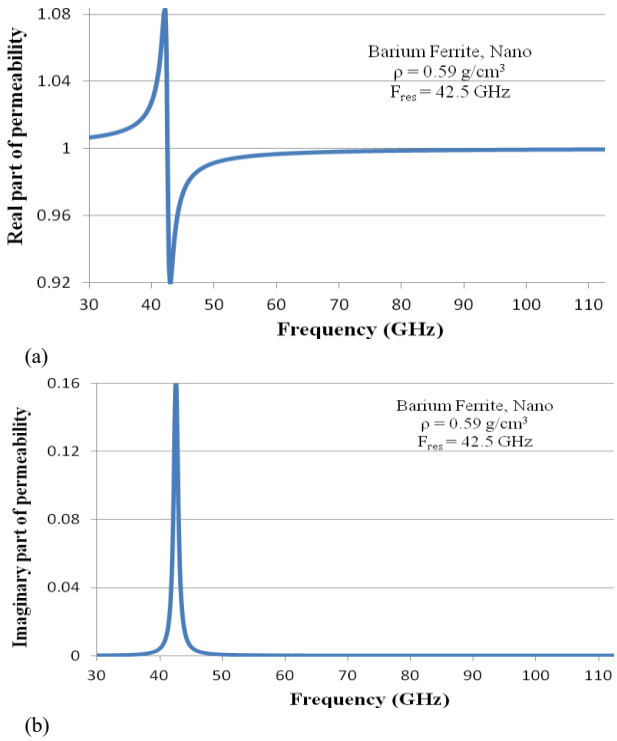

Fig. 12. Real (a) and imaginary (b) parts of permeability for Barium nano-ferrite powder measured in the millimeter wave frequency range.

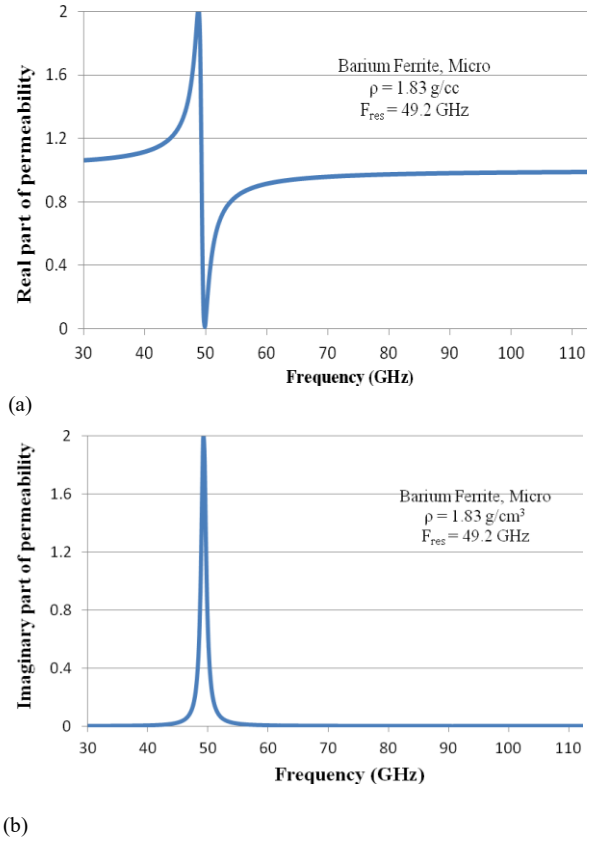

Fig. 13. Real (a) and imaginary (b) parts of permeability for Barium micro-ferrite powder measured in the millimeter wave frequency range.

A careful inspection of the plots in Fig. 12 and Fig. 13 lead us to conclude the best fit permeability values obtained in the lower frequency range (30 – 40GHz) are in good agreement with the values obtained from the microwave measurements. It is also observed that the micro-sized powders show higher values of intrinsic material properties as compared to the nano-sized powders in both microwave and millimeter wave frequency ranges.

An important observation from these plots concerns the resonance phenomena in these materials. It can be observed that the resonance frequencies are different for the two sizes of the powders. The resonance frequency seems to shift to lower values for nano-powders as compared to micro-sized powders. Resonance is the phenomena by which absorption occurs in ferrite samples. This means that the absorption frequency for a given composition of the ferrite sample can be tuned by changing the size of the particles in the sample.

IV. Conclusion

Microwave and millimeter wave properties of micro- and nano-size ferrite powders have been studied. Ferrites with different crystal structure and particle sizes have been studied. Measurement of samples in powder form is challenging at such high frequencies. Material characterization techniques were developed to accurately determine the intrinsic material properties, namely, permittivity and permeability of the powder samples. The network analyzer based microwave measurement technique has been modified to obtain precise measurements of material properties of powdered samples. Millimeter wave measurements have been performed by a quasi-optical spectrometer. Since the properties have been found to be size dependent, it is important that the measurement set-up is accurate enough to detect these differences.

The measurement of samples in powder form is a complex procedure. In the past, the powder samples have been diluted with conductive materials or epoxy to fabricate a solid sample for measurements. The procedure followed in this study does not use any such additive. Therefore the properties of the samples can be determined precisely. This information is useful to understand the behavior of the sample in the presence of electromagnetic energy. This knowledge can also be applied to simulate the material more accurately. Designers can save time and money by simulating their design before fabrication.

The results presented here reveal that the ferromagnetic resonance frequency of the ferrite samples varies with the particle size. Therefore the material can be tuned to resonate at different frequencies by changing the size of the particles. This is particularly useful in the design of high frequency tunable absorbers. The resonance observed in the case of nanoparticles is much sharper than that observed for bulk samples or samples containing micro-sized particles. Absolutely no resonance was observed in case of samples that did not contain the proper phase of barium hexaferrite. Preparation of ferrite powders in nano-size is challenging. The preparation procedure and conditions affect the properties of the sample. The techniques developed in this study can be used for non-destructive testing to check if the desired phase has been achieved or not. Accurate characterization would allow scientists to utilize nanomaterials to their full potential and achieve high performance in diverse applications.

References

[1] C. Buzea, I.I.P. Blandino, K. Robbie, “Nanomaterials and nanoparticles: Sources and toxicity,” Biointerphases, vol. 2, issue 4, pp. MR17-MR17, 2007.

[2] J. D. Adam, L. E. Davis, G. F. Dionne, E. Schloemann, S. N. Stitzer,“Ferrite materials and devices,” IEEE Transactions on Microwave Theory and Techniques, Vol. 50, No. 3, March

[3] U. Ozgur, Y. Alivov, H. Morkoc, “Microwave ferrites, part 1: Fundamental properties,” Journal of Material Science- Material Electronics, vol. 20, no. 9, pp. 789-834, 2009.

[4] M. Montrose, “EMC and printed circuit board- design, theory and layout made simple,”IEEE Press, 1999.

[5] Z. Peng, J.Y. Hwang, M. Andriese, “Microwave power absorption characteristics of ferrites,”IEEE Transactions on Magnetics, vol. 49, issue 3, March 2013.

[6] Z. Peng, J.Y. Hwang, M. Andriese, “Magnetic Loss in Microwave Heating”, Applied Physics Express, vol. 5, 027304, 2012.

[7] J. Thuery, E.H. Grant, “Microwaves: Industrial, scientific and medical applications,” 1992.

[8] L. Babes, B. Denizot, G. Tanguy, J. J. L. Jeune, P. Jallet, “Synthesis of iron oxide nanoparticles used as MRI contrast agents: a parametric study,” Journal of Colloid and Interface Science, vol. 212, pp. 474-482, 1999.

[9] J. H. Hafner, C. L. Cheung, A. T. Woolley, C. M. Lieber, “Structural and functional imaging with carbon nanotube AFM probes,” Progress in Biophysics and Molecular Biology, vol. 77, pp. 73-110, 2001.

[10] A. M. Attiya, “Nanotechnology in RF and microwave applications: review article”, 29th National Radio Science Conference, NRSC’2012, Egypt.

[11] A. M. Bhavikatti, S. Kulkarni, A. Lagashetty, “Characterization and electromagnetic studies of nano-sized barium ferrite,” International Journal of Engineering Science and Technology,vol. 2, issue 11, pp. 6532-6539, 2010.

[12] Afsar, Mohammed N., and Anjali Sharma. "Effects of Grain Size on Magnetic and Dielectric Properties of Ferrites at Millimeter-Wave Frequencies", IEEE Transactions on Magnetics, 2015.

[13] W. B. Weir, “Automatic Measurement of Complex Dielectric Constant and Permeability at Microwave Frequencies”, Proceedings of the IEEE, vol. 62, pp. 33-36, Jan. 1974.

[14] J. Baker-Jarvis, E.J. Venzura, and W.A. Kissick, “Improved Technique for Determining Complex Permittivity with the Transmission/Reflection Method”, IEEE Transactions Microwave Theory Tech., vol. 38, pp. 1096-1103, Aug. 1990.

[15] I. I. Tkachov, “Millimeter wave complex dielectric permittivity and complex magnetic permeability measurements of absorbing materials,” PhD. Dissertation, May 2000.

[16] T. Koutzarova, S. Kolev, C. Ghelev, K. Grigorov, I. Nedkov, “Structural and magnetic properties and preparation techniques of nanosized M-type hexaferrite powders,” Advances in Nanoscale Magnetism, Springer Proceedings in Physics, vol. 122, pp. 183-203, 2009.

[17] N. Dishovski, A. Petkov, I. Nedkov, I. Razkazov, “Hexaferrite contribution to microwave absorber characteristics,” IEEE Transactions on Magnetics, vol. 30, issue 2, pp. 969-971, 1994.

[18] S. Sugimoto, S. Kondo, K. Okayama, H. Nakamura, “M-type ferrite composite as a microwave absorber with wide bandwidth in the GHz range,” IEEE Transactions on Magnetics, vol. 35, issue 5, pp. 3154-3156, 1999.

[19] M.R. Meshram, Nawal K. Agrawal, Bharoti Sinha, “Characterization of M-type barium hexagonal ferrite base wide band microwave absorber,” Journal of Magnetism and Magnetic Materials, vol. 271, pp. 207, 2004.

[20] S.P. Ruan, B.K. Xu, H. Suo, F. Wu, S. Xiang, M. Zhao, “Microwave absorptive behavior of ZnCo-substituted W-type Ba hexaferrite nanocrystalline composite material,” Journal of Magnetism and Magnetic Materials, vol. 212, pp. 175-177, 2000.

[21] M. K. Tehrani, A. Ghasemi, M. Moradi, R. S. Alam, “Wideband electromagnetic wave absorber using doped hexaferrite in Ku band,” Journal of Alloys and Compounds, vol. 509, pp. 8398-8400, 2011.

[22] R. Sharma, R. C. Agarwala, V. Agarwala, “Development of electroless (Ni-P)/BaNi0.4Ti0.4Fe11.2O19 nanocomposite powder for enhanced microwave absorption,” Journal of Alloys and Compounds, vol. 467, pp. 357-365, 2009.

[23] S. P. Gairola, V. Verma, A. Singh, L. P. Purohit, R. K. Kotnala, “Modified composition of barium ferrite to act as a microwave absorber in X-band frequencies,” Solid State Communications, vol. 150, pp. 147-151, 2010.

[24] A. Ghasemi, A. Hossienpour, A. Morisako, A. Saatchi, M. Salehi, “Electromagnetic properties and microwave absorbing characteristics of doped barium hexaferrite,” Journal of Magnetism and Magnetic Materials, vol. 302, pp. 429-435, 2006.

[25] R.D.C. Lima, M.S.Pinho, M. L. Gregori, R.C.R. Nunes, T. Ogasawara, “Effect of double substituted m-barium hexaferrites on microwave absorption properties,” Materials Science-Poland, vol. 22, No. 3, 2004.

[26] A. Bahadoor, Y. Wang. M N. Afsar, “Complex permittivity and permeability of barium and strontium ferrite powders in X, Ku, and K-band frequency ranges,” Journal of Applied Physics, vol. 97, 2005.

[27] D. C. Kulkarni, V. Puri, “Perturbation of EMC microstrip patch antenna for permittivity and permeability measurements,” Progress in Electromagnetics Research Letters, Vol. 8, pp. 63-72, 2009.

[28] S. W. McKnight, L. Carin, C. Vittoria, S. F. Wahid, K. Agi, D. Kralj, "Picosecond-Pulse and Millimeter-Wave Spectroscopy of Barium Ferrite," IEEE Transactions on Magnetics, Vol. 32, No. 2, March 1996.
[29] N. Zeina, H. How, C. Vittoria, "Self-biasing circulators operating at Ka-band utilizing M-type hexagonal ferrites," IEEE Transaction on Magnetics, vol. 28, issue 5, sept 1992.
[30] B. Lax, K.J. Button, "Microwave Ferrites and Ferrimagnetics," McGraw-Hill, New York, 1962.

Wei. Quan received the B.S. Engineering degree from Shandong University in China in July 2010. He received MSEE from Tufts University in 2014. Presently he is working towards Ph. D. in Electrical Engineering at Tufts University. His current research includes Electrolyte (gel and solid) improvement, measurement instrument development.

Mohammed N. Afsar (F'89) received B.Sc (1965) and M.Sc (1967) degrees in Physics from University of Dacca, presently in Bangladesh He received M.S.E.E. degree from University College London of University of London in 1972. He received Ph.D. degree in 1978 from University of London, United Kingdom. He also worked as Higher Scientific Officer at the National Physical Laboratory, Teddington, United Kingdom from 1974 through 1978. He has worked as a Senior Scientist at MIT Francis Bitter National Magnet Laboratory from 1978 through 1984 in Cambridge, Massachusetts. He has been a full Professor of Electrical Engineering since 1984 at City College of the City University of New York. He moved to Tufts University, Medford, Massachusetts in 1987 as Professor of Electrical Engineering. He was the Chair of the ECE Department from 2004 to 2006. He became Fellow of IEE and Fellow of Institute of Physics in 1986 and Fellow of IEEE in 1989. He is now a Life Fellow of IEEE. He has worked in the development of Precision Electromagnetic Measurement Methods and Instrumentations at Microwave, Milliimeter Wave, Submillimeter and Terahertz Wave and on various Material Systems in all three phases. He has published about 360 technical papers and five edited books.